Agent-based model on resilience-oriented rapid responses of road networks under seismic hazard

Li Sun[1]; Dina D'Ayala[2]; Rosemary Fayjaloun[3]; Pierre Gehl[4]

[1] EPICentre, Department of Civil, Environmental & Geomatic Engineering, University College London, London, WC1E 6BT, United Kingdom (Email: li.sun@ucl.ac.uk);
[2] EPICentre, Department of Civil, Environmental & Geomatic Engineering, University College London, London, WC1E 6BT, United Kingdom;
[3] Department of Risks and Prevention, BRGM, Orléans, France;
[4] Department of Risks and Prevention, BRGM, Orléans, France.

Abstract: This paper explores a new pathway towards seismic resilience of Road Networks (*RNs*) under earthquake hazards, by leveraging post-shock rapid responses as the key to minimize the functionality losses of RNs, especially in the immediate aftermath of earthquakes. Accordingly, an agent-based modelling (*ABM*) framework is developed to enable the nuanced examination on resilience of earthquake-damaged RNs, when different system repair approaches are considered. In this framework, those different approaches are predicated on the damage level of individual bridges and on the system recovery timeline, i.e. the response to rehabilitation need is considered as a function of the time elapsed from the event. Each approach is represented by a different agent, whose behaviour is shaped by a set of pre-defined behavioural attributes, while the interplay among those agents is also accounted for, during the entirety of post-shock recovery campaigns. To demonstrate its applicability, the ABM framework is applied to a real-world RN across *Luchon, France*. As shown by the case-study, post-shock rapid responses are found to be a viable strategy to increase the recovery rate of RNs' functionality in the immediate-, and mid-term aftermath of damaging earthquakes, and ultimately, to improve the seismic resilience thereof.
Keywords: Seismic hazard; Resilience; Recovery; Rapid response; Partial repair; Road networks; Agent-based model

1. Introduction

The sustained functionality of modern road networks (*RNs*) is strategically crucial to the resilience of the urban communities that they serve, throughout destructive events, such as strong earthquakes (Gomez and Baker 2019). They become particularly vital across mountainous regions, where they might represent the only means of mobility for the residents to connect to other communities and to access critical services, in the aftermath of damaging natural hazards. Nonetheless, *RNs* in such locations have proven to be insufficiently robust, as demonstrated by real-world seismic events, around the globe (Zhao and Taucer 2010, Lekkas et al. 2012). Furthermore, the protracted disfunction of *RNs* is often found to have a significant knock-on effect on all facets of the emergency response, across the affected region (D'Ayala et al. 2019), and the restoration of the other interconnected critical infrastructure systems (Zhao and Sun 2021).

As one of the most important components of modern *RNs*, the functionality of bridges under earthquake hazards is critical to seismic resilience of the whole system. Decò et al. (2013) proposed a probabilistic model to assess seismic resilience of bridge structures. Following such

a model, the initial damage induced by earthquake hazards is evaluated by fragility functions of the bridges of interest. To deliver the adaptive recovery associated with different levels of initial damage and different pace of rehabilitation operations, a probabilistic six-parameter function was proposed as a viable tool to shape the recovery path of bridge structures.

Resilience assessment of *RNs*, has also been conducted at system level. Guidotti et al. (2017) studied the system reliability of *RNs* under seismic hazards. To that end, in their model, the seismic fragility of *RNs* has been examined on both the nodal and system level, considering four different connectivity measures (i.e. diameter, efficiency, eccentricity and heterogeneity), in the wake of damaging earthquakes. Do and Jung (2018) considered the societal impacts of seismic resilience of *RNs* on the community they serve. To that end, a quantitative evaluation method is developed and applied to the *RN* in Sejong city, South Korea. The work highlights the need to restore *RN* functions in a priority-based order. Specifically, to maximize the traffic-carrying capacity of the whole *RN*, it is preferable to restore road sections based upon users' priority, rather than investment costs. Kilanitis and Sextos (2019) have developed a holistic framework for the multi-criterion assessment and management of seismic risk and resilience of *RNs*. Both the structural and monetary losses, along with the broader financial, connectivity and environmental impact of hazard levels with different annual rate of exceedance are put into context and employed to gauge the seismic resilience of *RNs*. Such a framework can therefore enable the stakeholders to device cost-effective strategies to ameliorate seismic resilience of *RNs*. Most recently, Wu et al. (2021) proposed a modelling framework on the long-term recovery of *RNs*, under earthquake hazards. In such a framework, a resilience indicator was introduced and employed to balance the trade-off between the overall travel time and safety performance of earthquake-damaged *RNs*, and a bridge restoration prioritization index was generated accordingly. Therefore, such a framework can help to develop long-term recovery plan for *RNs*, with the presence of some partially functional bridges.

In light of the complex dynamics associated with the recovery of the *RN-Community Systems*, the agent-based model (*ABM*) approach has been leveraged as an adaptive tool to dissect and model resilience behaviour of those socio-technical networks (Ouyang 2014). Sun et al. (2019a) proposed an *ABM* framework for assessing seismic resilience of the integrated system of *Road Network-Power Network-Community*. Based on the case-study, it was found that the interplay among operators of different *CISs*, who are modelled as the agents, can profoundly affect the recovery trajectory of such interwoven socio-technical networks. Furthermore, the outcome also indicates that sluggish restoration of individual *CIS* can have a significant "bottleneck" effect on the recovery of others connected to them. Hence, a well-

coordinated restoration of interdependent *CISs* was found to be one of the most crucial parameters in determining the resilience of the whole system.

Notwithstanding the increased interest in use of advanced stochastic and *ABM* techniques to determine the resilience of *RNs* exposed to natural hazards (Argyroudis et al. 2020), with very few exceptions (Shao et al. 2018), little attention has been paid to the decision-making in the immediate aftermath of earthquakes (*IAoEs*), although it is generally recognised that such early decisions shape the whole recovery process (Hassan and Mahmoud 2020). The trajectory of the recovery process for road networks, as a measure of their resilience, is proposed by Zhang et al. (2017).

Against this backdrop, as a research endeavour to deliver tools for the resilience improvement of socio-technical systems, through better exploitation of post-shock rapid responses, this paper focusses on how the implementation of the rapid response on the earthquake-damaged bridges can expedite the recovery of road networks and minimise the corresponding disruptions to the urban community. To that end, in this study, an adaptive and compositional modelling framework has been proposed, to enable seismic resilience modelling of *RNs*, and the examination of the effectiveness of the rapid-response. In such a framework, the initial *functionality loss* of any branch of the *RNs* immediately following seismic hazards is quantified by linking it to the probability of physical damage of any bridge on that branch, expressed through fragility functions for different damage levels. Beyond the absorption phase, their functionality trajectory throughout the post-shock recovery phase, including *IAoEs*, is shaped by the developed agent-based model (*ABM*). Several indicators are used to measure the level of resilience of the *RN* under different scenarios of increasing magnitude. It is found that the physical resilience of the network, is very sensitive to small changes in magnitude with a strongly non-linear behaviour. This is even more apparent when the societal impact is measured through the restoration time for the connectivity of the critical path. Moreover, the study demonstrates that the looped interdependence between the post-shock rapid response and the regular repair procedure of damaged bridges is critical to the recovery trajectory of *RNs*, in the immediate-, and mid-term aftermath of damaging earthquakes, which substantially affects seismic resilience of the *RNs*. Under an earthquake scenario with the maximum magnitude M_w = 7, the post-shock rapid responses can reduce the restoration time of critical connectivity of the *RN* by up to 96.8%, if self-reliant.

The remainder of the paper is organised as follows. *Section 2* first introduces a conceptual modelling framework which situates this rapid response-based resilience approach within the wider context of damage recovery of complex urban systems, and how it is influenced and

influences the community recovery and resilience. Following such a framework, an agent-based model (*ABM*) for seismic resilience of *RNs* is proposed and elaborated on, in *Section 3*. The proposed *ABM* framework is applied to a real-world *RN* in *Bagnères-de-Luchon, France*, whose seismic resilience is investigated from both the physical and societal perspectives, in *Section 4*. The case-study outcome demonstrates the applicability of the proposed *ABM* framework to real-world cases and highlights the need for further developments. *Section 5* draws the main conclusions and sheds light on the potential pathways forward.

2. Rapid response-based resilience (*RRbR*) of modern *CISs*

The modus operandi of urban communities is underpinned by an array of Critical Infrastructure Systems (*CISs*), which have become increasingly interdependent and interwoven, through sharing and exchange of the operation resources and information (Kröger and Zio 2011). Such a transformation is contributing to the efficient functioning of *CISs*, however, also renders those systems more vulnerable to disruptive events, such as strong earthquakes (Helbing 2013).

Against this backdrop, post-shock resilience of those interwoven *CISs* has become strategically crucial to the well-being of the whole community that they serve (Guidotti et al. 2019). Conceptually, resilience is characterized as the capacity of *CISs* to absorb the effects of a disruption to their performance, referring to robustness, yet more, to recover that performance, in a swift and sound pattern (Bruneau et al. 2003, Hosseini et al. 2016). Standard modelling of seismic resilience of interconnected system of *CISs* assumes that the restoration of their functionality starts when all damage induced by the earthquake hazards has been "absorbed" (Argyroudis et al. 2020). In general, studies are focussed on the overall measure of functionality loss of the system (Bruneau et al. 2003, Ouyang et al. 2012, Sun 2017), rather than its rate of change throughout the recovery. Nevertheless, many of the lessons learnt from past seismic events have highlighted that one of the main deficiencies regarding state-of-the-art resilience modelling frameworks lies in their lack of characterization of the criticality associated with different time-windows, throughout the post-shock recovery stage (Aydin et al. 2018).

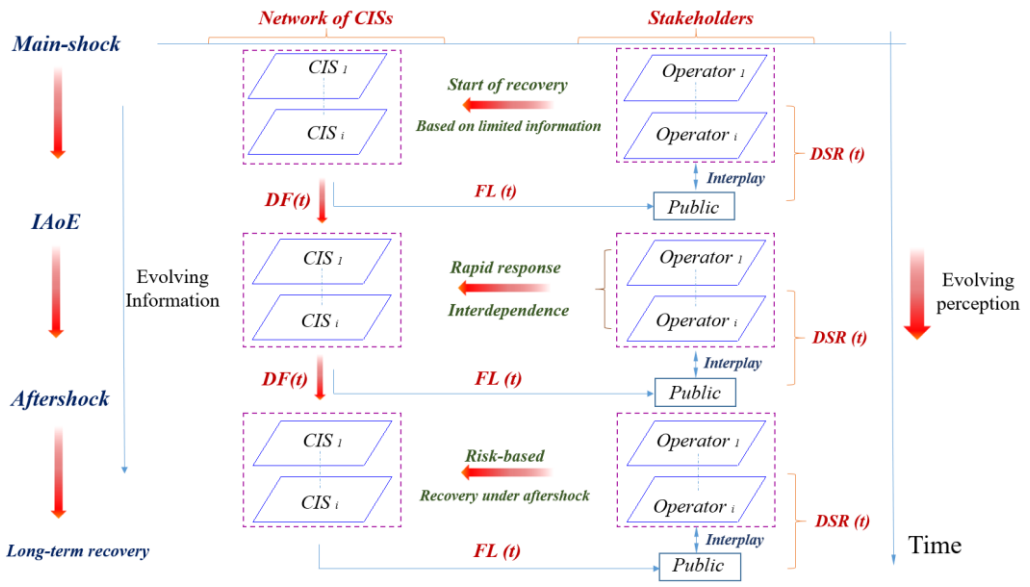

Figure 1. Time and information dependent recovery of interconnected critical infrastructure systems (*CISs*) subject to seismic hazards. *DF(t)* stands for deliverable functionality, *FL(t)* for functionality loss, *DSR(t)* is the dynamic stakeholder response.

Figure 1 shows the proposed conceptual framework, which contextualises the recovery of a system of a set of the interwoven *CISs* within modern communities, affected by the time-varying information, perception and level of hazard. The purpose of such a framework is also to highlight the research needs for the rapid response-oriented recovery. Within the framework, the post-shock recovery of *CISs* can be disaggregated into three sub-stages characterised by different conditions:

The immediate aftermath of earthquakes (***IAoEs***): During this stage, potentially with large number of casualties and widespread earthquake-induced and cascading damage to buildings and *CISs*, the primary objective is to restore the functionality of *CISs* to a minimum acceptable level, so that the emergency rescue, evacuation and sheltering can be delivered. However, due to the incomplete and inaccurate information during such a stage, it is challenging for *CISs Operators* to react in an expeditious and well-coordinated way. Typically, protocols are followed based on the level of pre-event preparedness of the specific organisation. Meagre research has been conducted on this phase so far. Fraioli et al. (2021) use a discrete-event system approach to identify key factors that would have a significant impact on the restoration time, and emphasized that the disaster managers of *CISs* should hoard sufficient volume of emergency-response resources, at all times.

Recovery under (potential) aftershock sequences: Real-world earthquake events are often characterised by mainshocks followed by aftershock sequences with damage potential, which usually decreases in magnitude and frequency obeying known seismological patterns, but could also increase (Reasenberg and Jones 1994). Dong and Frangopol (2015) developed a detailed

framework for the computation of mainshock-aftershock sequence effects on the repair costs and functionality losses of bridges, outlining how this can influence the decision-making on post-event repair/rehabilitation activities to reduce economic and societal impacts considering full event sequences, but also determine the decisions on network access (Alessandri et al. 2013).

Long-term recovery: Throughout such stages, considerable social and business activities will restart and be likely affected by the post-shock restoration and reconstruction endeavours. Overall, long-term reconstruction of severely damaged *CISs* components will take a long time, and shall be planned pursuant to the socio-economic demand across the affected communities. Gyawali et al. (2020) suggested that the promotion of *Sustainable Livelihoods* for those earthquake-affected communities shall be perceived as the highest priority to be addressed throughout such stages. To that end, economic rejuvenation, sustainable use of natural resources, and participatory demand from different sectors shall all be promoted and facilitated.

The decision-making on specific activities related to the post-shock recovery throughout the three stages identified in Figure 1, is dependent on the *Dynamic Stakeholder Response* (*DSR*), which is essentially driven by the evolving perception of the gap between the deliverable functionality (*DF*) of *CISs*, and the concurring demand from the end users (Sun et al. 2015, Aki 2017). *DSR* is highly dependent on information availability and flow, which increases in quantity and quality throughout the event sequence. Blake et al. (2019) examined the flow and use of information during the response and recovery decision-making across all transport modes in the aftermath of the M_w 7.8, 2016 Kaikōura earthquake, New Zealand. While many positive aspects in the communication flow were identified, one observation critical to this study is that the actors on-the-ground, managing the repairs, were not engaged directly in the communication chain, notwithstanding their critical position, to provide real-time insights while responding to highly dynamic situations, where uncertainty is significant and decisions are needed immediately. Many of the real-world catastrophic earthquakes have highlighted the far-reaching impact of the lack of expeditious post-shock responses on seismic resilience of the whole system of Community-*CISs*, throughout the three stages discussed above. For instance, in the aftermath of April 25, 2015 Gorkha earthquake in Nepal, while the bridge infrastructure exhibited a good response, the road network was highly affected by earthquake induced landslides and rockfalls in the foot hills. This was extended by the 12 May aftershock and the recovery of the road network in the following months was severely hindered by the monsoon season, having a detrimental effect on the hydropower plants recovery, and in turn on households' recovery throughout the affected region (Hashash et al. 2015). Much of this

evidence is however anecdotal and a systematic analysis framework of the whole phenomenon is not available.

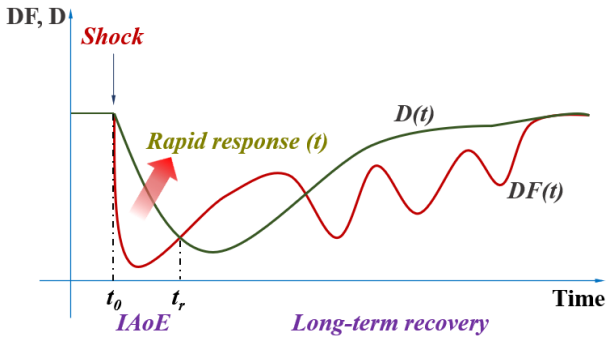

Figure 2. Modelling framework on rapid response-based resilience (*RRbR*) of modern *CISs*.

Therefore, in this paper, a modelling framework for *Rapid Response-based Resilience* (***RRbR***) of *CISs* throughout seismic events is proposed. In such a framework, the post-shock recovery phase will be subdivided into two stages, namely, the immediate aftermath of the earthquakes (*IAoEs*), and the long-term recovery thereafter. As illustrated in Figure 2, the time points t_0 and t_r denote the moment when the seismic event occurs, and the end of the *IAoEs*, respectively, which indicates that the system has recovered sufficiently, to satisfy the reduced demand of the post-shock state of the community (e.g. reduced need of mobility because of the closure of school, factories and etc.). Clearly, the duration of *IAoE* is case-specific, as it is dependent on the magnitude of the seismic event, the specific physical vulnerability of the system, and the societal context of *CICSs* (SPUR 2009, Smith 2013).

Correspondingly, for each *CISs*, it can be postulated that, as shown in Equation (1):

$$RR = \text{argmin}\left(\int_{t_0}^{t_r}(D(t) - DF(t,a))dt\right) \quad (1)$$

defines the rapid response (*RR*) as the set of actions taken by the *Operator* of each individual *CIS* to minimize the functionality deficit throughout the *IAoEs*, where *D(t)* refers to the functionality demand, while *DF(t, a)* denotes the recovering deliverable functionality, conditioned on the action *a* taken by the *Operator*.

3. Agent-based Model on *RRbR* of *Road Networks*

Within this study the functionality of the *RNs* is examined in the separate *Absorption*, *Immediate Aftermath of Earthquake (IAoE)*, and *Long-term recovery* stages, respectively. Essentially, the focus during the *Absorption* stage lies in the estimation of the functionality losses of *RNs* immediately following the shock. Afterwards, as shown in Figure 3, throughout the ensuing *IAoE*, the *ABM* will be employed to examine how the functionality restoration of *RNs* is shaped by both the *rapid-response* and *regular repair*. In this paper, the post-shock

rapid response is defined as the set of activities to restore the functionality of the earthquake-damaged bridges to an incomplete, yet minimal acceptable level, whereby the emergency rescue and evacuation could be delivered. In practice, given the structural characteristics of the damaged bridges, such rapid responses could usually be implemented by building temporary bridges, ramps or bypasses (Schanack et al. 2012, Durante et al. 2018), or delivering the *rapid repair* of critical damaged members (Parks et al. 2016, Sun et al. 2017). In the following case-study, the *rapid response* will only be delivered to those bridges with severe damage. Ideally, rapid responses should be delivered in a few days. Although specific time frames for rapid repair delivery are not clearly defined in practice, current research aims at interventions to be accomplished by squads of two people within 24 hours (e.g. Fakharifar et al. 2016). However, from the real-world perspective, such endeavours tend to be encumbered by the widespread damage of the *RN*, as well as the interaction with the other interdependent *CISs*, throughout *IAoEs*. From evidence available in literature, it is realistic to assume that it would take around a week to complete a rapid response on a critical bridge (Durante et al. 2018, Norton 2020). Conversely, *regular repair* refers to the set of actions typically employed to deliver the full restoration of the functionality of the damaged bridge, irrespective of its level of damage.

Beyond the rapid response phase, the functionality of the whole *RNs* will be restored by the regular repair alone, in the long-term recovery stage. In this study, only the damage of bridge structures will be considered, whereas those road segments connecting them are assumed to be intact. This is justified by the large number of bridges of different configurations and seismic performance, present on the network under study, and by its topology. In the following the specific modelling of each stage is discussed.

3.1 Absorption stage

The earthquake-induced functionality losses regarding various bridges of *RNs* is quantified by considering seismic functionality-loss functions. Mathematically, such functions provide a measure of the probability that the bridge of interest could retain a certain fraction of their pre-shock functionality, conditioned on the intensity measure of the earthquake ground motion at its geographic site, obtained from seismic attenuation models. Nonetheless, for real-world bridge structures, the quantitative relationship between the seismic damage they have sustained and the corresponding loss of functionality is indeed complex and very case-specific (Gehl and D'Ayala 2016, Gehl and D'Ayala 2018). To address such a challenge, in this paper, seismic fragility functions are employed to determine the *Damage States* (*DSs*) of bridges under seismic hazard. A total of three *DSs* are considered, i.e. no damage (*DS1*), minor damage (*DS2*), and extensive damage (*DS3*). The seismic fragility model developed by Shinozuka et al. (2002)

is employed for beam bridges, while the fragility functions published by Zampieri (2014) is used to model the response of arch bridges. The vulnerability of the bridge is then assessed by quantifying its remaining degree of functionality, given its *DS*. The bridge functionality loss metrics proposed by Gehl and D'Ayala (2018) is employed in this study. Following such metrics, it is assumed that bridges with *DS3* are completely closed to vehicular traffic, while those bridges with *DS2* are set to remain passable, but the travelling speed on them will be reduced to 25% of the pre-shock level. In the following, it is assumed that two operators are collaborating to restore the network: a rapid response operator, who might represent a *Civil Protection Agency*, tasked with leading activities in the emergency and immediate aftermath phase, represented by Agent A; and a recovery operator, representing the conventional network management agency, which will dispatch two different agents, B and C, tackling bridges with minor and severe level of seismic damage, respectively, to reflect the different level of resources needed and consequences for the network functionality.

3.2 Immediate aftermath of earthquake

Once the probabilistic damage states of each of the individual bridges have been determined, conditional to the particular earthquake scenario, *RNs* will enter *IAoEs* (Figure 2). As discussed in *Section 2*, the ultimate objective of rapid response throughout such a stage is to restore the traffic-carrying capacity of *RNs*, in particular, the connectivity of a set of critical paths, to an acceptable level. However, the time needed to fulfil such objectives can be very case-specific. In this paper, the time span of such a stage is set to be one month, with regard to earthquake scenarios with the maximum magnitude, by which time the full functionality of the majority of those severely-damaged bridges will very unlikely be restored (Decò et al. 2013), but the restoration on the connectivity of critical paths through rapid responses, can be accomplished. A multi agent-based model is proposed in this study, as an adaptive and inclusive modelling strategy, with regard to the interacting post-shock *rapid response* and the *regular repair* of *RNs* (Sun et al. 2019b), to investigate whether such a time frame is realistic, when applied to a real-case scenario, given the current data on repair and replacement delivery. Previous studies have looked into the prioritization of bridge repair on the basis of various criteria (Merschman et al. 2020), nonetheless, the working assumption being that the repair phase occurs by considering one bridge at a time. In the present study, three different *Repair Unit Agents* have been considered to model the restoration of bridges, as discussed in the previous section. The behaviour of those agents throughout the recovery campaign is shaped by a set of pre-defined behavioural attributes.

In each realization of the simulation following the *Absorption* stage, the *Agent A* delivering the post-shock *rapid-response* throughout *IAoEs*, will start the *rapid response* on the damaged bridges, without any idle period.

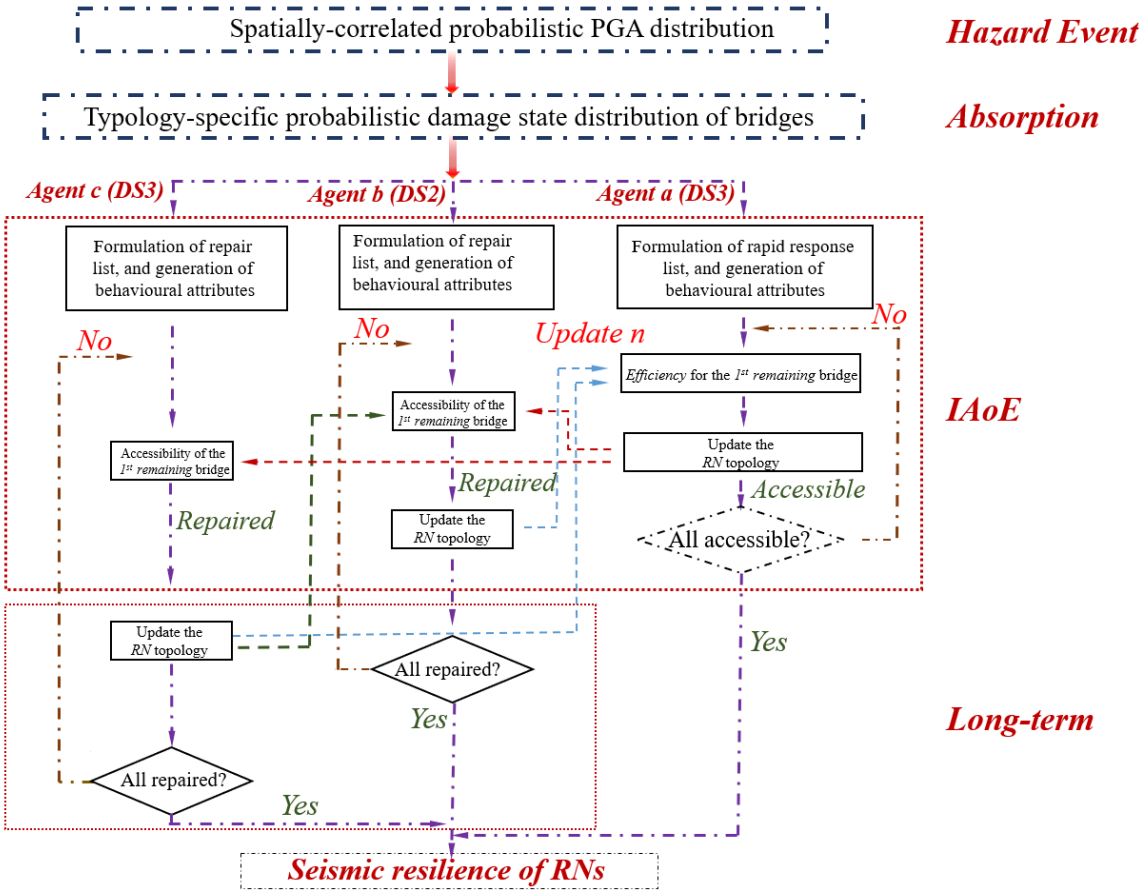

Figure 3. Process of recovery as modelled through the concurrent activity of rapid response agent and repair agents.

Agent a will only intervene on those bridges with *DS3*, in light of their critical impairment of accessibility to other critical services (e.g. hospitals and emergency shelters), and their potentially long-lasting bottleneck effect on the repair of other bridges with *Minor damage* (*DS2*).

It shall be noted that, it would be rather challenging to formulate the optimal rapid response sequence of repair to a *RN*, following catastrophic earthquakes. Regarding a local *RN* like the one considered in the following case-study, for earthquake scenarios with high magnitude and epicentre close to its central area, approximately 16% of the bridges would be severely damaged, say 19 bridges. Accordingly, there would be 19! (= *1.2165e+17*) permutations of possible sequences. Therefore, the use of a basic optimization routine would be unfeasible on any real-world problem, as also recognised by Bocchini and Frangopol (2012). Instead engineering reasoning is used in this paper to plan rapid responses, based on the network and

bridge characteristics. Technically, it will be increasingly difficult to provide promptly temporary replacement bridges in the form of prefabricated ramps or spans to create bypasses, for bridges with span length greater than 50m (Yeh et al. 2015), due to local logistics and procurement delays. Indeed, Long et al. (2013) proposed a system for construction of temporary arch bridges, which can take few days for spans up to 10m. Therefore, in this paper, as a straightforward criterion for rapid response priority at system level, the bridges with *DS3* are ranked based on their span, as a measure of ease of reparability, in the ascending order.

The initial number of bridges with either *DS2*, or *DS3*, will affect the pace of delivery of the *rapid response* in the *IAoE* phase, and the rate of restoring access for each individual bridge, depending on its position on the ranking list and its span. Therefore, as shown in Figure 3, the start time and completion time of the *rapid repair/replacement* of each bridge (out of a total of N_r ones) is defined by Equations (2-4):

$$R_{r,j} = T_{r,j} + \frac{F_{r,j}}{E_r * \omega^n} * \frac{\text{Span(j)}}{50}, \quad \text{if } Span\ (j) \leq 50\text{m or}$$
$$R_{r,j} = T_{r,j} + \frac{F_{r,j}}{E_r * \omega^n} * \left(\frac{\text{Span(j)}}{50}\right)^2, \quad \text{if } Span\ (j) > 50\text{m}, \tag{2}$$

with $j = 1: N_r$ and

$$T_{r,1} = SD_{r,0}/V_r \tag{3}$$
$$T_{r,j} = SD_{r,j}/V_r, \quad for \quad j = 2: N_r \tag{4}$$

where $T_{r,1}$ is the time required to start the repair of the first bridge, since the seismic event. Given the *RN* topology, the travelling time between the *rapid response* centre and the first bridge (*i.e.* the severely-damaged bridge with shortest span) is set to be determined by the length of the shortest path between the two locations (denoted as $SD_{r,0}$); V_r is the travelling speed of the rapid response team, which is a function of the path maximum allowed speed, including speed restriction on slightly damaged bridges. The total time needed to deliver the rapid response on the first bridge, denoted as $R_{r,1}$, will thereby be obtained by $T_{r,1}$ plus the required repair time as defined in (Eq. 2).

In Eq. (2), $F_{r,1}$ denotes the component functionality objective to be restored, which in the *IAoEs* is set to be the target of being accessible, with the corresponding travelling speed set to be 10% of the pre-shock level; E_r denotes the efficiency of the *rapid repair/replacement* squad, also treated as a probabilistic variable. To account for delays associated with the network typology and topology, with initial lack of information on actual damage, as well as the availability of resources, need for clearance operations, etc, as shown in Eq. (2), the efficiency

parameter is reduced by a factor ω^n (ω<1), where ω is a pre-defined reduction coefficient, while $n(t, b_d, b_t)$ denotes the number of damaged bridges (with either *DS2*, or *DS3*) associated with the shortest path between the last bridge that the Agent A has delivered the rapid response (denoted as b_d), and the one it is heading to tackle (denoted as b_t) . As shown in Figure 3, n will assume a new value for each rapid response loop, and will depend on the number and location of bridges repaired by the other two agents.

Moreover, for each individual bridge *j*, according to Eq. (2), the *repair/replacement time* will increase linearly with its span, denoted as *Span (j)*, when shorter than 50m, while it will increase quadratically with *Span (j)*, if longer than 50m.

The model described above therefore allows to develop a looped interdependence between *rapid repair/replacements* and *regular repairs*. The expeditious rapid response will help to alleviate the bottleneck effect with regard to the regular repair, which will in turn, accelerate the rapid response itself.

3.3. Long-term recovery

As shown in Figure 3, following the *Absorption* phase, like *Agent A*, also *Agent B* and *Agent C*, will be dispatched to deliver the *regular repair* on damaged bridges with *DS2* (i.e. minor damage), and *DS3* (i.e. severe damage), respectively. Both agents formulate their repair sequences by ranking the bridges based on their *betweenness centrality*, with the assumption that the topology of the road networks affects the efficiency of restoration. Mathematically, the betweenness centrality of bridge v is computed following Equation (5):

$$g(v) = \sum_{s \neq v \neq t} \frac{\sigma_{st}(v)}{\sigma_{st}} \quad (5)$$

where σ_{st} is the total number of shortest paths from node s to node t, and $\sigma_{st}(v)$ is the number of those paths that pass through v (Brandes 2001). A ranked repair list can therefore be generated in descending order, based on such a criterion, and each of the two *Agents B* and *C* will depart from the *Repair Centre* and start to repair the first bridge on their own repair list (i.e. the bridge with the largest value of betweenness centrality, with regard to both *DS2* and *DS3*). Similar to Equations (2) ~ (4), the repair time for each bridge with *DS2* will be determined by the two behavioural attributes of the agent, namely, V_m and E_m, which refer to the traveling speed of the *Agent B* and its repair efficiency, respectively. Hence, for each individual bridge *i* with *DS2* (the total amount of which will be denoted as N_{DS2}), the time needed to start and finish its repair will then be determined following Equations (6) ~ (8):

$$T_1 = T_0 + SD_0/V_m \quad (6)$$

$$R_i = T_i + F_{m,i}/E_m \,, \; i = 1: N_{DS2} \quad (7)$$

$$T_i = R_{i-1} + SD_i/V_m \,, \; i = 2: N_{DS2} \quad (8)$$

where T_1 is the time needed to reach the first bridge, since the seismic event. Similar to Eq. (3), SD_0 refers to the length of the shortest path between the *RN* repair centre and the first bridge (in the specific ranked repair list), given the *RN* topology, which is different from the pre-shock one, and is itself a function of the repairs undertaken at any given time. Therefore, for the first bridge, the corresponding travelling time will be obtained by SD_0 divided by the attribute V_m, which again is affected by the restriction on speed on any of the bridges with *DS2*. Besides, T_0 is set to consider the time for the *Agent B* to scheme the repair plan, while preparing the necessary repair resources (Decò et al. 2013, Sun et al. 2019b). The total time required to restore the functionality of the first bridge, denoted as R_1 can therefore be obtained by T_1 plus the required repair time quantified *by* $F_{m,1}/E_m$. Here, $F_{m,1}$ denotes the functionality to be fully restored, for the first bridge. In this case, full restoration of functionality responds to the criteria of the bridge being passable with the pre-shock allowed speed level, i.e. means that all lanes have been restored and therefore no speed or weight restrictions are in place. The *Agent B* will proceed to restore the next bridge in the repair list, until the functionality of all bridges with *DS2* has been fully restored. Nevertheless, it shall be highlighted that *Agent B* would likely encounter inaccessible paths, due to the existence of bridges with *DS3*. Regarding such cases, in this study, before being able to reach a particular bridge scheduled for the repair, *Agent B* is assumed to be waiting until the restoration of the accessibility of those severely-damaged bridges (*DS3*), which occlude its available path forward to such a bridge, delivered by either *Agent A* (rapid response), or *Agent C* (full repair). Finally, the Agent C's behaviour will be modelled in the same way as *Agent B*, yet with different behaviour attributes, namely, V_s and E_s, respectively. However, as the complete functionality recovery (defined as stated for *DS2* bridges) on most of the bridges with *DS3* would only be delivered in the long-term recovery stage (Figure 3), when calculating the travelling time, the potential bottleneck effect from those bridges with *DS2* will be considered only in the earlier phase of activity of *Agent C*, namely, during *IAoEs*.

3.4 Multidimensional resilience measures

In order to quantify the seismic resilience of *RNs* from both the physical and societal point of view, a total of three resilience measures are proposed in this study:

A. *Functionality losses at the component level.* As already stated, the only components of *RNs* analysed in this paper are the bridge structures. It is justifiably important to first examine the probabilistic distributions of *DSs* associated with individual bridges, particularly, those critical ones with high betweenness centrality, or those ones that are most vulnerable to

seismic hazards. Only the damage distribution obtained in the absorption stage following the main shock is investigated in this study. In other words, the influence of aftershock events (during the recovery phase, shown in Figures 1 and 2) on the *DSs* of bridges will not be modelled in this paper;

B. *Percentage of functional bridges*, denoted as *PFB(t).*

$$PFB(t) = \frac{\sum_{i}^{B_{tot}} f(i,t)}{B_{tot}}, \text{ with } f(i,t)=1, \text{ if functional; Otherwise, } 0 \quad (9)$$

As shown by Eq. (9), at any given time *t*, *PFB(t)* can be examined, based on the functionality state of each individual bridge *i*, denoted as *f(i,t)*. The value of *f(i,t)* is set to be *1*, if the bridge has no damage or if it has been fully repaired. Otherwise, it equals to *0*. *PFB(t)* will be monitored throughout the entirety of the recovery phase, and employed as a physical resilience measure at the system level;

C. Normalized length of critical path, denoted as *NLCP(t).*

$$NLCP(t) = \frac{LCP_{orig}}{LCP(t)} \quad (10)$$

The ultimate role played by *RNs* is to enable the uninterrupted mobility of people. It is self-evident that the traffic-carrying capacity of *RNs* is contingent not just upon the *PFB*, but also the topology of *RNs*. Throughout the recovery phase, the *RNs'* topology itself will evolve over time, affected by the shock sequence and the corresponding repair and rapid response. By the end of the *Absorption* phase, some of the road segments of *RNs* will be inaccessible, due to the damage or collapse of one or more bridges associated with them. From the perspective of graph theory, the *RN* topology then is different from the one at the pre-shock stage, as those inaccessible road segments are essentially removed from the topological model representing the *RNs*. Given the start and end nodes of interest, the shortest path between them may likely be substantially different from the one obtained before the earthquake event, or there might not be any accessible path anymore. However, upon the start of the *IAoEs*, the functionality of those damaged bridges will start to be restored. Those inaccessible paths can thereby be available again, as those associated damaged bridges have been partially or fully repaired. Therefore, in this study, the topology of the system is reanalysed after each rapid repair/replacement or regular repair has been completed, and the shortest path between that particular pair of start and end nodes is updated (i.e. shortened, or fully restored to the original one associated with the intact *RN*). As shown in Eq. (10), the global dynamic behaviour of the *RNs* is therefore well interpreted by the *normalized length of critical path* (*NLCP*) of interest. Here, LCP_{orig} and *LCP(t)* refer to the geographic length of that particular path, obtained from the original topology and the time-varying topology, at time point *t* following the earthquake hazard, respectively. From

a socio-economic perspective, the length of the set of critical paths of *RNs* will be strategically crucial to the emergency aid, the evacuation of the wounded, as well as the restoration on several other interconnected *CISs*, as mentioned in *Section 2*.

4. Case study

4.1 Configuration of the case-study RN

To examine the adaptability of the modelling framework proposed and the effectiveness of rapid responses, the *ABM* developed hereinbefore is applied to a real-world *RN* across the *Luchon Valley, France*, a historic and touristic region, one of the valleys of the *Pyrenees* connecting France to Spain. Such a hierarchical *RN* consists of a *route nationale* (*N125*), several *route départementales*, and rural roads. Given the mountainous topography and the presence of several water courses, the *RN* comprises 118 bridges, of which 89 beam-type bridges, 1 truss bridge and 28 arch bridges, and connects 53 municipalities (small villages and towns), as shown in Figure 4.

4.2 Scenario-based simulation following the developed ABM framework

On account of the significant uncertainties with regard to seismic hazards, as well as the vulnerability and recovery behaviour of *RNs*, *Monte Carlo* (*MC*) simulations are run to account for their collective influence on the seismic resilience of the *RN*. The simulation outcomes presented hereinafter are obtained from *2,000 MC* simulations. For each realization, the simulation is run for a reference time of 1,800 days, to ensure the full recovery of the network and repair of all damaged bridges. As the post-shock recovery continues, the state of the *RN* is updated at each time step, set as half day, allowing the whole recovery trajectory to be tracked.

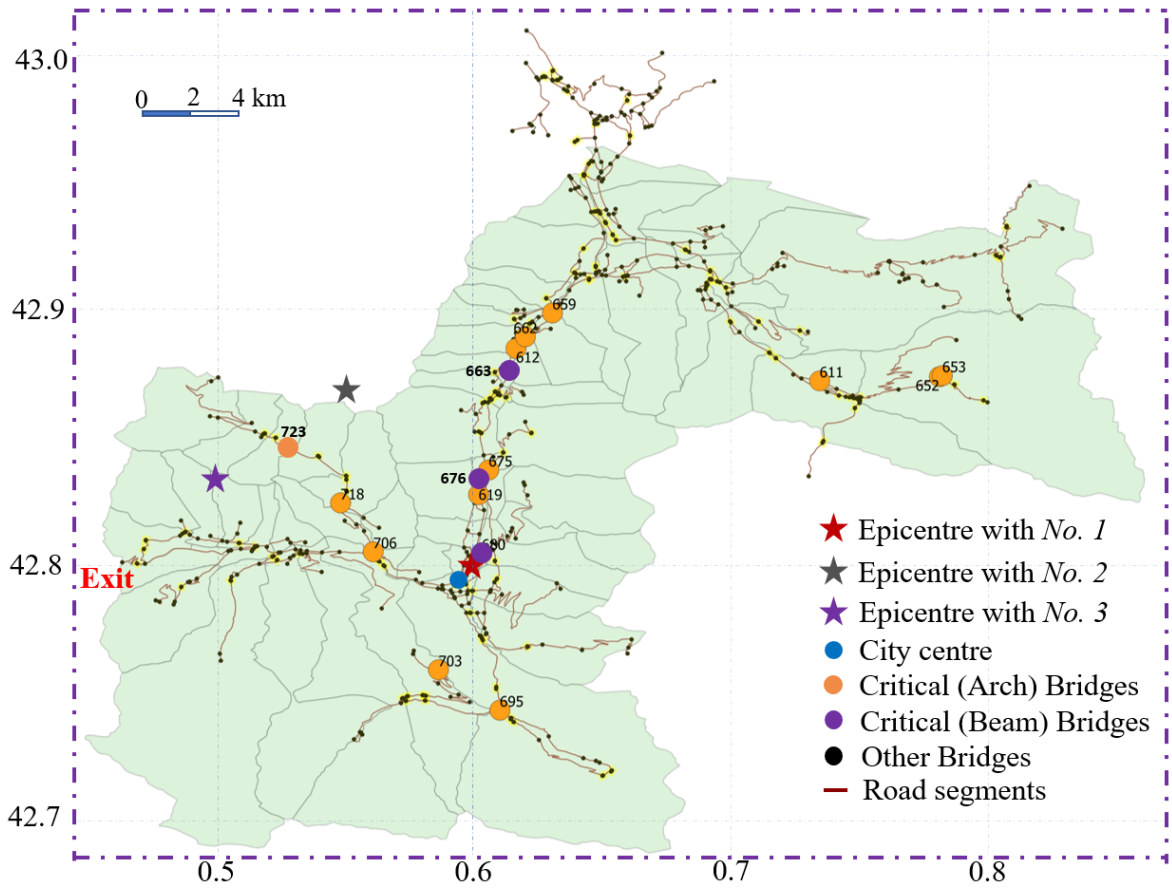

Figure 4. Topology of the road network in *Luchon*, France.

The realization of each single *MC* simulation is set to start with the generation of an earthquake scenario, characterized by the location of its epicentre and the corresponding seismic magnitude M_w. On the basis of recorded historic seismic activity across the region, three epicentres close to the central area of *Luchon*, with coordinates presented in Table 1, are considered in this case-study, as shown in Figure 4.

Table 1. Location of epicentres.

Epicenter	Longitude (*W*)	Latitude (*N*)
1	0.6	42.8
2	0.55	42.867
3	0.5	42.833

To generate ground shaking scenarios, different ground motion models have been considered as recommended by García-Fernández et al. (2019), ultimately choosing the ground motion attenuation model for a rock site proposed by Campbell and Bozorgnia (2008), applicable to earthquake scenarios with Mw≤ 7.5. Given the upper limit of the *SHARE* seismic source area model across the region (Woessner et al. 2013), the maximum seismic magnitude considered in this paper is set to 7.

For each single bridge of the RN, its DS is determined by fragility analysis, based on the Intensity Measure (IM) of the ground motion at its geographic location, obtained from the attenuation model.

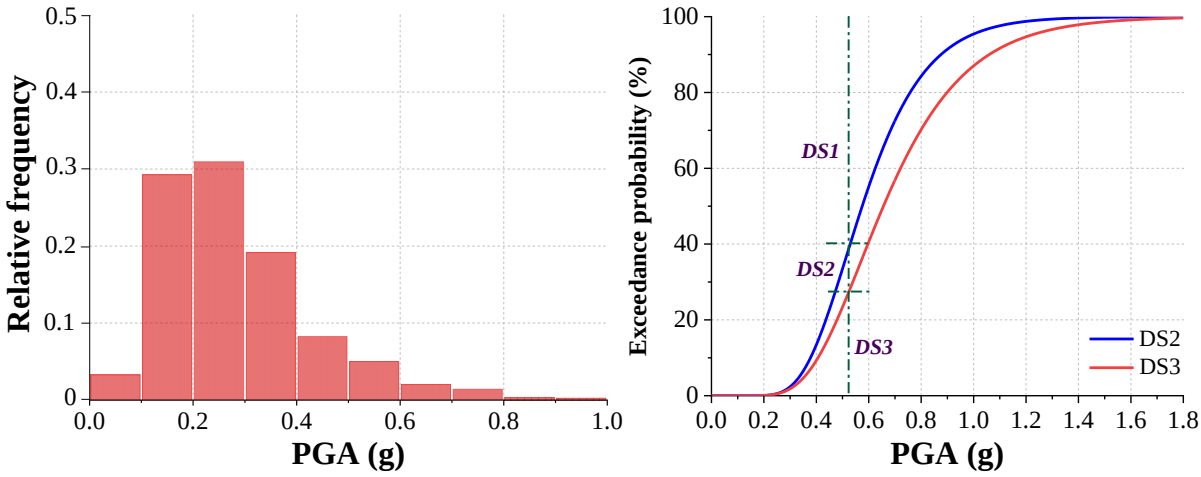

(a) PGA histogram (b) Fragility functions for a specific bridge type

Figure 5. Probabilistic distribution of intensity measure at one critical bridge location as sampled through the MC simulation and the corresponding fragility functions.

Figure 5 shows the histogram of the *Intensity Measure* (e.g. *Peak Ground Acceleration*) at the geographic site of bridge *#663* for a scenario with the epicentre No.1 and magnitude M_w=*7*, and the corresponding fragility behaviour for such a bridge. It shows that the value of the resulting *PGAs* is varying between *0.2g* and *0.4g*, for the majority of the realizations. It can be further found that, given its fragility function, for such a range of *PGA* values, the probability of being in *DS2* or *DS3* are low but not insignificant, from the probabilistic point of view.

The functionality losses associated with each earthquake-damaged bridge can be determined, based on its *DS* obtained from the fragility analysis. Accordingly, the trajectory of their post-shock functionality recovery, driven by the activity of those three *agents* described above, can also be tracked thereafter. To that end, in each of the simulations, the behavioural attributes of those agents will be randomly generated following the probabilistic distributions, characterized by the pre-defined parameters, presented in Table 2. Specifically, for *Agent A*, the travelling speed (V_r) is set to follow a uniform distribution with the lower and upper limits of *15km/h* and *20km/h*, respectively. Such a relatively low speed is assumed, to account for the potential impact of the debris and jam on the travel, throughout the *IAoE* phase, in an implicit way. Accordingly, the lower and upper limit for the travelling speed (V_m) of *Agent B* in charge of the repair on bridges with *DS2*, who may need to ship some heavier equipment, are set to be *5km/h* and *10km/h*, respectively, while the travelling speed V_s of *Agent C* delivering the

restoration of bridges with *DS3*, is set to be varying between 2.*5km/h* to *5km/h*, assuming that major on-site equipment will need to be mobilised for each repair.

In terms of *Efficiency*, for *Agent A*, E_r is set to follow a uniform distribution with lower and upper limit of 100/day and 200/day, respectively. This means that the time needed to complete the rapid response for a single bridge will range from 0.5 to 1 day. However, it is noteworthy to highlight that, as shown in Eq. (3), such a time will be increasing with span length, linearly up to 50 m, and then quadratically, for spans exceeding 50m. More importantly, E_r will also be reduced by the factor ω^n (ω<1), as explained in *section 3*.

For *Agent B* and *Agent C*, their *Efficiency* parameters (denoted as E_m and E_s, respectively) are also assumed to be following uniform distributions. The corresponding lower and upper bounds of such distributions are summarised in Table 2.

Table 2. Behavioural attributes of the three *Agents*

Attribute	Lower	Upper	Distribution	Average recovery time
V_r (km/h)	15	20	Uniform	0.75 day
E_r (%)	100	200	Uniform	
V_m (km/h)	5	10	Uniform	15 days
E_m (%)	5	10	Uniform	
V_s (km/h)	2.5	5	Uniform	60 days
E_s (%)	1.25	2.5	Uniform	

4.3 Simulation results

As mentioned hereinbefore, resilience of the *RN* in *Luchon* will be investigated from the perspective of the probabilistic *DSs* of critical bridges, *PFB(t)*), and *NLCP(t)*, respectively. To that end, a graph-theory (topological) model is established to represent such a *RN*, where each individual node refers to a starting/end point, while the links among them are set to represent the corresponding road segments. In total, there are 682 edges, and 607 nodes, as shown in Figure 6.

Based on that graph, the betweenness centrality of each single bridge can therefore be computed following *Eq. (5)*, which will serve as the measure of the criticality of the *118* bridges of the *RN*. However, to account for the hierarchical nature of the *RN*, with greater traffic capacity and demand on the national road and substantially lower traffic capacity on the local roads, the betweenness centrality of bridges, associated with the "regional" and "local" road systems, is scaled down by 0.1 and 0.01, respectively, while the betweenness of bridges belonging to the "main" road system is kept unchanged. Based on the scaled betweenness, two bridges with *ID* No. *663* and *676*, become the two most relevant ones (Figure 4), with regard

to the whole *RN* (i.e. with the highest betweenness centrality values). Indeed, they are both located on the national road connecting the central and northern regions of *Luchon*.

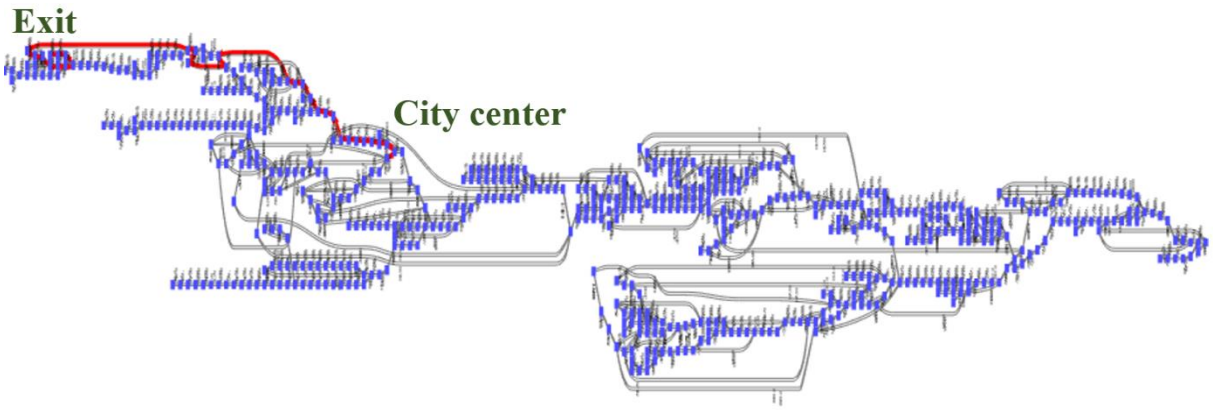

Figure 6. Graph-theoretical model of the *RN*.

To determine the efficiency of the repair and the restoration of critical paths, after analysing a number of critical Origin-Destination pairs, the start and end node have been set to be the city centre and the southwest exit of the *RN*, which links the valley's population to critical emergency facilities (see Figure 4). The shortest path between these two nodes is 11.5 km, given the topology of the intact *RN*.

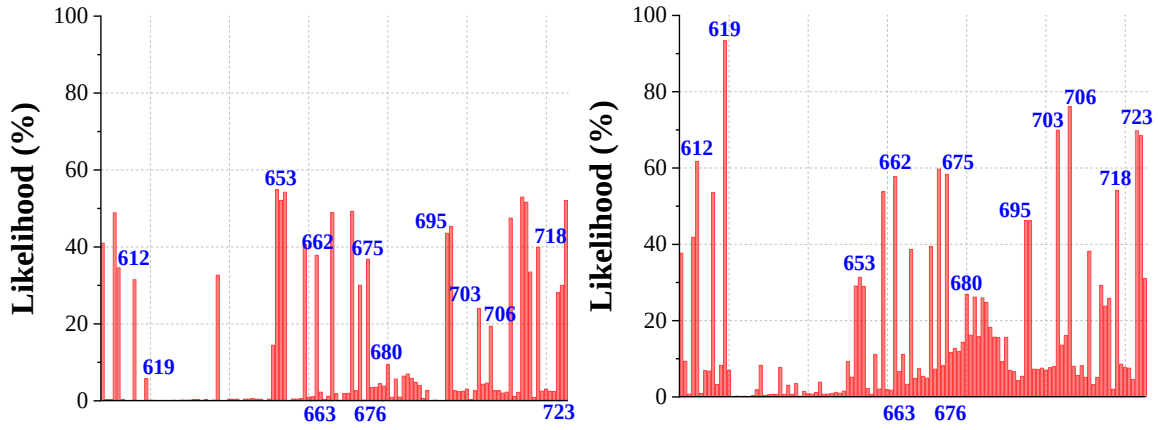

(a) DS2 (b) DS3

Figure 7. Damage Sate of critical bridges under seismic scenarios with different magnitude.

The stochastic analysis under M_w *7* scenarios (with epicentre No.1) obtained through the 2000 MC realisations provides a probabilistic distribution of the damage states *DS2* and *DS3* for each of the 118 bridges, as plotted in Figure 7, which can be interpreted together with their betweenness centrality ranking to determine critical bridges across the network and the critical paths. For instance, regarding bridge *#663*, its likelihood of *DS2* and *DS3* are found to be merely *2.25%* and *6.65%*, respectively. It shall be noted, in light of its high betweenness centrality, the seismic robustness of this bridge is strategically valuable, as many of the paths

can thereby be maintained, notwithstanding widespread damage across the *RN*. The analysis shows that for the specific level of magnitude chosen, the maximum credible in the region, the likelihood of *DS3* is significantly larger than that of *DS2* for many bridges. Among all, due to its proximity to the epicentre, bridge *No. 619* turns out to be the most vulnerable one, in terms of *DS3*. It can be noted that several masonry arch bridges have high probability of being in *DS3*, and as mapped in Figure 4, they would affect both the national and regional branches of the network, and substantially affect the mobility throughout the valley and its accessibility, as for instance bridge *No. 706*, being on the critical path between the city centre and the exit.

The results on recovery and restoration of the chosen critical path are presented in the following considering two distinct scenarios: first, a conventional recovery process, considered as the baseline scenario, where only *Agent B* and *Agent C* are active; then a second scenario, which considers the activity of all three *Agents* and determines the gain to be had by implementing rapid repair/replacements in the *IAoE* period.

A. Baseline scenario: conventional recovery process

In Figure 8, the sensitivity of seismic resilience of the *RN*, with regard to different locations of the epicentre was first examined, by tracking the median of its *PFB(t)*, under scenarios with M_w*=7*. In general, the recovery trajectories are not found to be radically different from each other, despite the different location of epicentres and different initial number of non-fully functional bridges. Specifically, for the epicentres with Nos. 1, 2 and 3, the *PFB* value is found to be 73.7%, 76.3%, and 78.0%, respectively. In light of the same probabilistic distribution of the behaviour attributes of the agents (Table 2), the overall recovery rate of the *RN* is close to each other, regarding all the three epicentres. Eventually, it takes *1023* days, *962.5* days, and *840* days, respectively, for the *RN* to be fully recovered.

Given the similarity of the resulting resilience of the *RN* with regard to different epicentre locations, the behaviour of the *RN* is further investigated, under the scenario with *Epicentre No.1* alone, which induces the most serious damage, on the systems level.

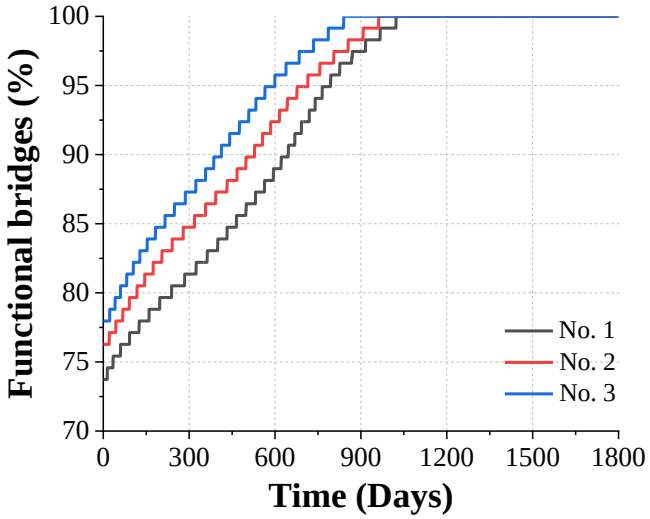

Figure 8. Median *PFB(t)* under earthquake scenario with different epicentres.

Figure 9(a) tracks the median *PFB(t)* of the *RN*, under earthquake scenario with different magnitudes. The analysis at network scale shows the sensitivity of seismic resilience of the *Luchon RN* to the increasing magnitudes. Specifically, its median *PFB* in the absorption phase drops from 90.7% to 73.7%, as the magnitude increased from 5 to 7. Similarly, the median full recovery time vary from 191 days to 2.8 years for the same range of magnitudes. It should be noted that the rate of recovery is not substantially affected by the increase in magnitude although two step changes can be seen between M_w 5.25 and M_w 5.5 and between M_w 6 and M_w 6.5, corresponding to increases in the number of bridges with *DS3*.

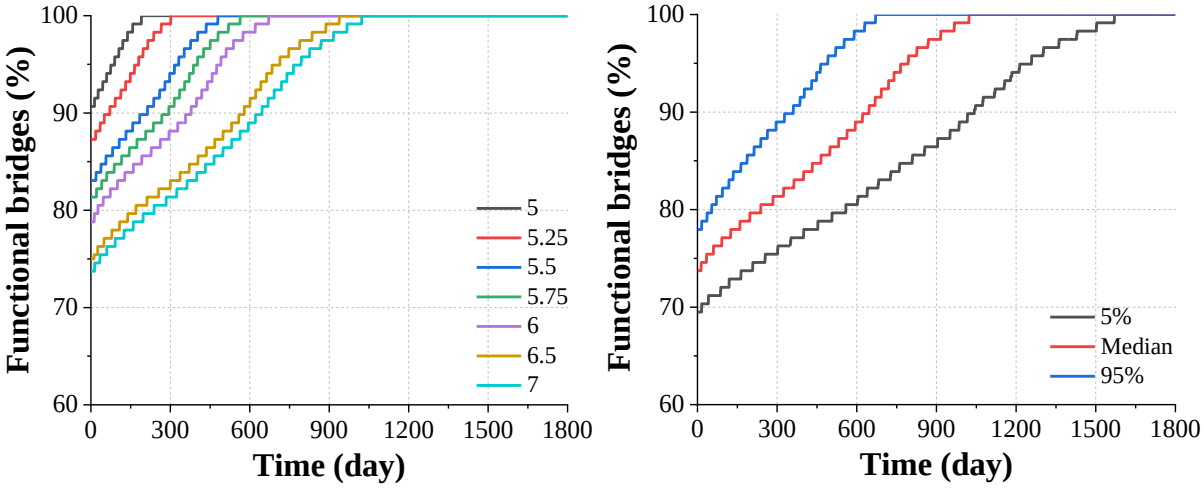

(a) Median resilience under scenario with different magnitudes (b) 5% and 95% quantiles under $M_w = 7$

Figure 9. *PFB(t)* under earthquake scenario with different magnitudes.

In Figure 9(b), the quantile of 5% and 95% of the *PFB(t)* under seismic scenario with M_w=7, are also presented. It should be noted that even considering the hazardous event as a given scenario, the stochasticity regarding seismic resilience of the *RN* is large, due to the collective

impact of the uncertainty associated with seismic fragility of the bridge structures, their recoverability, and the interdependences thereof. The uncertainty of seismic fragility is measured by the *PFB* immediately following the shock, which is found to be ranging between 68% and 78%. On the other hand, it can be seen that the recovery paths diverge with time, and for the 5% quantile, it will take up to 4.3 years to fully repair all the seismically-damaged bridges. Such a significant lack of resilience, notwithstanding the fairly low exceedance likelihood, underscores the sensitivity of the system to the uncertainty associated with the recovery behaviour, and the importance to define them more accurately.

To further examine the recovery trajectory of bridges with different *DSs*, Figure 10 presents the time-varying number of bridges with *DS*2 and *DS3*, respectively, under scenarios with different magnitude. It can be found that, immediately following the seismic hazard, the number of bridges with *DS3* will be growing from 3 to 19, as the magnitude is increased from 5 to 7, while the recovery rate remains constant throughout. For the same range of scenarios, the number of bridges with *DS2* increases from 8 to 12. The pattern associated with their post-earthquake recovery, however, are fairly different. Notwithstanding the same behavioural attributes, the stagnancy regarding the recovery is found to be increasingly pronounced, as the magnitude increases, due to the bottleneck to recovery induced by the increase of the amount of bridges with *DS3*, which prevents reaching bridges with *DS2* conditioned on certain branches of the network until they have been fully repaired.

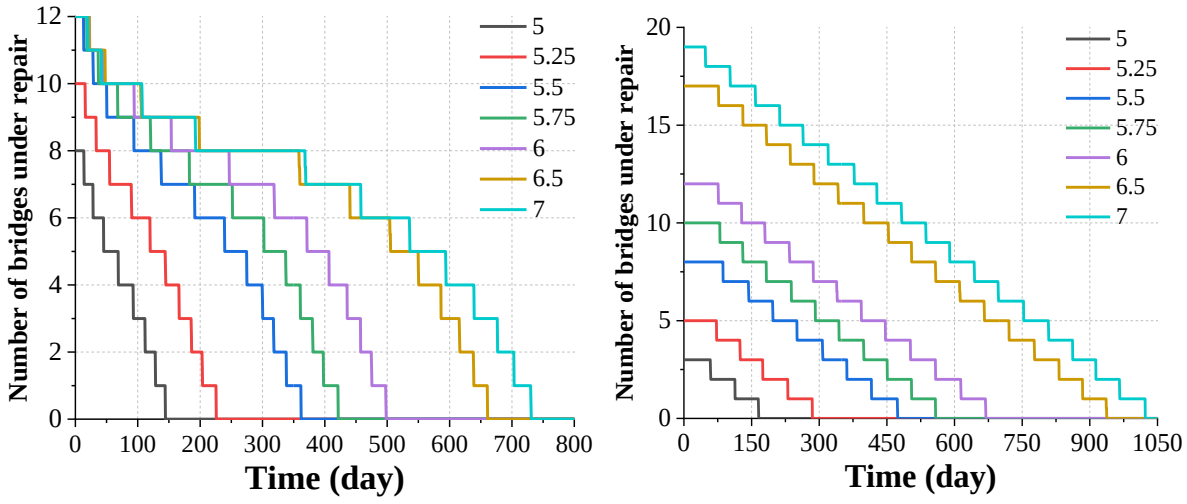

(a) DS2 (b) DS3

Figure 10. Median number of bridges under seismic scenarios with different magnitude.

In Figure 11, the *NLCP(t)* between *City Centre* and *Exit* (Figure 4) under those different earthquake scenarios are tracked. Results show that the *NLCP* is not substantially affected by earthquakes of magnitude lower than 5.5, so that the corresponding recovery time is almost 0,

even though the number of damaged bridges is non-zero. This highlights that, although the network is highly hierarchical and has a substantially in-series layout, there is nonetheless sufficient redundancy to accommodate up to 13% of the bridges being damaged, with 5 of them seriously, without losing accessibility.

However, once the magnitude reaches the threshold of 5.5, the response of the *RN* turns out to be substantially different, as no available path can be identified between the pair of nodes of interest anymore (thus 0, in Figure 11) following the shock. More crucially, such a loss of connectivity remains unchanged for *76.5* days. This outcome reveals that as the number of non-functional bridges increases, the system-level resilience would degrade, given its topology. For magnitudes increasing from 5.75 to 7, no accessible path can be determined between the two reference points for up to 81.5 to 109.5 days, which suggests a long-lasting functionality loss, and the associated socio-economic disruptions. It shall be noted that, as shown in Figure 4, such a particular path connects the city centre to an exit of the valley, which will thereby be employed to transport the wounded to the hospitals, to evacuate the affected inhabitants, and to ship the emergency necessities. Such a lack of societal resilience would thus pose a strategic risk to the whole community, under hazardous events, especially, in the *IAoE* phase.

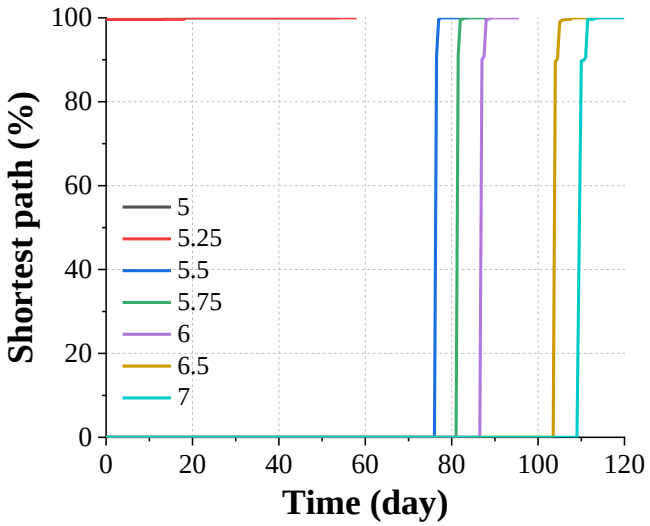

Figure 11. Normalized, median *NLCP* under seismic scenarios with different magnitude.

B. Rapid Response Scenario

The simulation outcome presented above has highlighted that, the *RN* of interest will not be sufficiently resilient under strong earthquakes, particularly from the societal perspective. Therefore, the post-shock rapid responses should be leveraged as an alternative pathway to the enhancement of seismic resilience of earthquake-damaged *RNs*. However, justifiably, for the increased widespread damage inflicted to the network, the delivery of *Rapid Response* will also be increasingly encumbered. Therefore, to simulate such a dependency of the rapid response

on the level of seismic damage in the *IAoE* phase, and the concurrent regular repair activity, the factor ω is employed as a multiplier of the efficiency parameter and assigned values ω = *0.5*, *0.75*, and *1*, respectively. The higher the ω value is, the more self-reliant the *Rapid Responses* will be, and for ω = 1, there is no hindrance on the activity of *Agent A*. Moreover, as described in *Section 3*, another parameter *n*, which is the exponent of ω and denotes the number of damaged bridges associated with the path to the next target bridge in the *IAoE* phase, will also be introduced to account for that dependency.

Additionally, the duration of *IAoEs* in this *paper*, as already mentioned in *Section 3*, is set to be 30 days, following the main shock.

Figure 12 examines the influence of parameter ω, on the *Rapid Response* itself. In the case of ω = *0.5*, the benchmark efficiency E_r will therefore be reduced by 0.5^n, so that the rapid repair/replacement is found to be delivered to only 8 bridges, by the end of the *IAoE*. The partial restoration of accessibility of the limited amount of bridges with *DS3* is thus expected to be unable to substantially expedite the regular repair on bridges with *DS2*. In particular, as mentioned in *Section 3.2*, the guiding strategy of the rapid response *Agent* A is to address the restoration of the "easiest" bridges first, so as to maximise the number of passable bridges in the short term. However, such bridges might not be necessarily on those paths to be taken by the *Agent B*, whose sequence is ranked by betweenness centrality of the bridges of *DS2*.

This outcome also highlights the difficulty of delivering rapid responses in a really "rapid" way, unless the influence of the widespread damage of the *RN* can be mitigated through "pre-emptive" preparedness, for instance, by appropriately distributing the resources needed for post-shock rapid responses, such as enough vehicles able to carry heavy equipment and prefabricated metal ramps, across minor roads, through the mountainous valley.

As the ω value increases, the influence of regular repairs on the activity of *Agent A* is less pronounced. From Figure 12, in case of ω = *0.75*, all bridges with damage *DS3* can be made passable within the rapid response timeframe of 30 days, with a single delay identified by the plateau observed. Moreover, as showed in Table 2, on average, it will take around *15* days and *60* days to fully restore one bridge with *DS2* and *DS3*, respectively. Therefore, according to Figure 12, the rapid response has already been delivered to the majority of bridges with *DS3* on the 15^{th} day, which means that the corresponding bottleneck effect could be effectively lifted, before the completion of the regular repair of the first bridge with *DS2*.

Finally, for ω = *1*, not only the rapid response can be delivered to all the severely-damaged bridges, but also is unaffected by the existence of the other damaged bridges of the *RN*, as $1^n = 1$. Therefore, as shown in Figure 12, the rapid response trajectory is nearly a straight line and

the entirety of the rapid response campaign takes only *10.5* days. While this situation is clearly ideal, the fact that the average repair time is 15 days for the first bridge with *DS2*, means that there is negligible difference in terms of *RN* resilience associated with the two cases of ω = *0.75* and *1*, respectively.

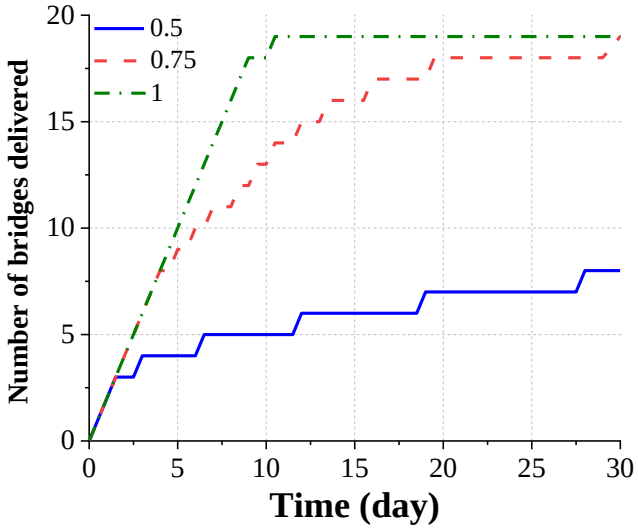

Figure 12. Median number of bridges with rapid response delivered, under seismic scenarios with magnitude 7 for different values of ω.

In Figure 13, the resulting functionality trajectories of the whole *RN*, as well as the recovery path of bridges with *DS2*, under the earthquake scenarios with the magnitude of 7, associated with three different values of ω, are tracked and compared with the outcome obtained from the baseline case without *Rapid Response*.

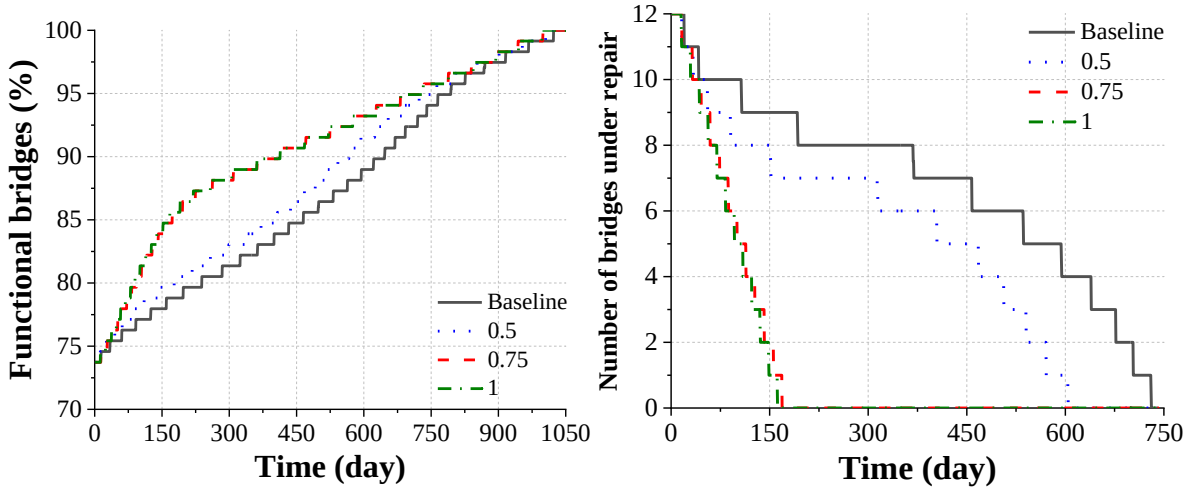

(a)Functional bridges (b) Bridges with DS2

Figure 13. Median trajectory under seismic scenarios with magnitude 7.

It can be found that, compared with the baseline case, the *Rapid Responses* is able to improve seismic resilience of the *RN*, yet by a narrow margin, when ω = *0.5*. In terms of the

repair on bridges with *DS2*, the overall recovery rate is indeed slightly higher than that of the baseline. Nevertheless, it shall be noted that the plateau observed in Figure 10(a) can still be found, which indicates that the repair on bridges with *DS2* would still be impeded by the bottleneck effect from some bridges with *DS3*. The whole recovery campaign (on bridges with *DS2*) is thus only shortened by *17.3*% (from *731* days to *604.5* days).

As ω reaches 0.75, however, the resulting resilience behaviour is found to be sharply enhanced. Figure 13(a) shows that the overall recovery rate substantially increases since the very beginning of *IAoE*. Compared with the baseline, it can be found that the time needed to reach *85%* of the pre-shock level has been reduced by *62.8%*, i.e. from *465.5* days to *173* days. The positive interaction between *Agent A* and *Agent B* is demonstrated by Figure 13(b), whereby the plateau observed in the first two cases can no longer be identified, showing that the *Agent B* is no longer hindered by damaged *DS3* bridges. Finally, it only took *169* days to fully repair all the bridges with *DS2*, which account for *23.1%* of the time needed for the baseline case.

When the rapid response become completely "independent" ($\omega = 1$), the seismic resilience of the *RN* is not further improved, in a significant way. From Figure 13(a), it took *167.5* days to reach 85% of the pre-shock level. In terms of those bridges with *DS2*, the entirety of the recovery campaign took *162* days, signifying a *77.84*% reduction, compared to the baseline.

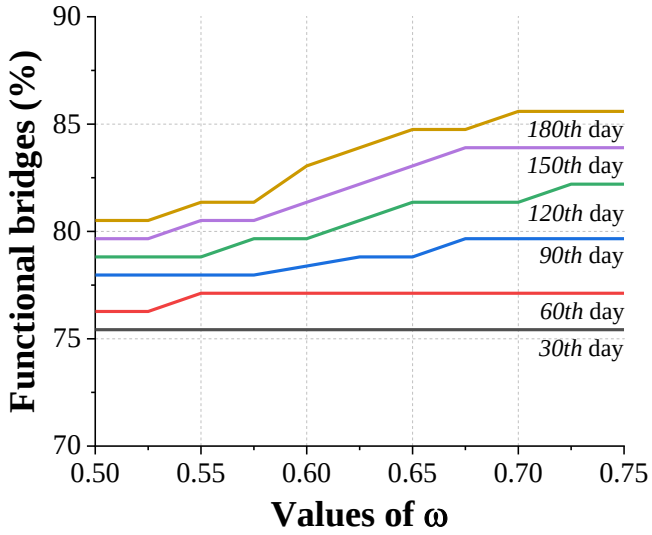

Figure 14. Median *PFB* on "milestone" moments under earthquake scenario with magnitude of *7*, given different ω values.

To further examine the influence of ω on *the* seismic resilience of the *RN*, in Figure 14, the median *PFB* on a set of "milestone" moments (which includes the 30^{th}, 60^{th}, 90^{th}, 120^{th}, 150^{th}, and 180^{th} day after the earthquake), have been tracked by the additional simulations with ω value increased from 0.5 to 0.75, with the step of 0.025. Overall, it can be found that, for the

first two moments, *PFB* is found insensitive to different ω values, consistent with the observations from Figure 13. Therefore, although the rapid response campaign concludes on the 30^{th} day, it is too soon for its beneficial effect to be observed, given the average rate of repair for bridges with either *DS2*, or *DS3* (Table 2). However, the resilience improvement become increasingly pronounced, from the 90^{th} day onwards. It can be seen that the growing value of ω lead to a steady increase of the percentage of functional bridges. Specifically, on the 120^{th} day, there is an increase of 3.4% of functional bridges between the cases with ω =0.55 and ω =0.725 (also shown in Figure 13). Such a pattern holds true and becomes more remarkable, when it comes to the response of the *RN*, on the 150^{th} and 180^{th} days, respectively. For the former, an increase in the ω from 0.525 to 0.7 yields an increase of *PFB* from 79.66% to 83.9%, in an almost-monotonical way, while an increase from 80.5% to 85.6% of *PFB* is measured on the 180^{th} day for the same change in the value of ω. From the perspective of risk governance, such an observation indicates that, even the slight increase of self-reliance of the rapid response unit, e.g. through the improved preparedness, could substantially improve the seismic resilience of *RNs*.

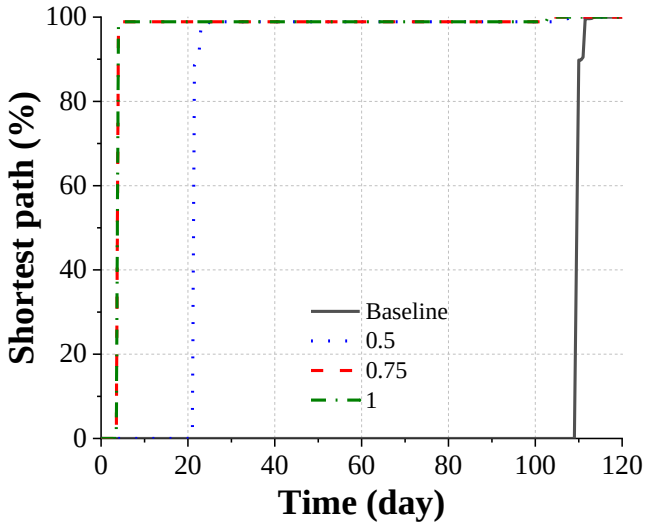

Figure 15. Median number of the *NLCP* under seismic scenarios with magnitude 7.

Finally, Figure 15 examines the *NLCP* of interest, regarding the four different cases. It is shown that the rapid response can significantly accelerate the restoration of the connectivity of such a path. Even for the case of ω = 0.5, accessibility of the critical path can be restored *88* days earlier (*21.5*th day versus *109.5*th day), despite the marginal contribution made by the rapid response, regarding the recovery rate of the percentage of fully functional bridges (Figure 13(a)). In particular, the corresponding period is further shortened to *3.5* days, as ω reaches 0.75 and 1, respectively. Such a reduction by up to 96.8% is strategically critical, not only to

the emergency aids and evacuations, but also to the restoration on other *CISs*, which will in turn, have a knock-on effect on seismic resilience of the *RN* itself.

5. Conclusions and Outlook

Road Networks (*RNs*) are strategically critical to seismic resilience of the whole community that they serve, under damaging earthquakes. Nevertheless, real-world seismic events around the globe have demonstrated that *RNs* themselves are often insufficiently robust, and thus impair access to critical services, as well as the recovery on a host of other interconnected Critical Infrastructure Systems (*CISs*), in the immediate aftermath of earthquakes (*IAoEs*).

Current resilience modelling frameworks of *CISs* available in literature focus mostly on the total functionality losses of *CISs*, throughout the entirety of the absorption and recovery process of a catastrophic event, without characterizing the criticality of different time-windows and the associated activities. In this paper, however, it is revealed that an expeditious post-hazard functionality restoration in the immediate aftermath of those events, even if only partial, indeed plays a strategically crucial role with regard to the global resilience of *CISs*. Furthermore, the study conducted in this paper also shows that it is possible to use engineering criteria to determine a generic model of recovery that can provide case specific and case sensitive results. This can therefore allow the applications in practice, which can support decision-makings based on the modelling and the quantification of the improved resilience.

Accordingly, an agent-based modelling (*ABM*) framework has been developed to enable a nuanced modelling on the rapid response-based seismic resilience of *CISs*, considering different repair strategies in relation to different phases in the recovery process and different level of damage of the assets. To demonstrate its applicability, the framework is applied on a real-world Road Network (*RN*) in *Luchon*, France. Seismic resilience of such a *RN* is quantified, using both physical and social metrics. The impact of different earthquake scenarios and the interdependence between the regular repair and rapid response on seismic resilience of the *RN* is examined in detail, and the following conclusion can be drawn:

1. The granularity of the proposed *ABM* framework enables the formulation and quantification of *RNs*' resilience measures, which are crucial to the governance policy on seismic risk of modern communities;

2. Seismic resilience of the *RNs* is found to be profoundly influenced by different earthquake scenarios. In particular, the societal resilience of *RNs* could sharply decay and thus pose a significant seismic risk to the entire community, as the magnitude of the earthquake hazards reaches a certain threshold value;

3. A looped interdependence between the post-shock rapid response and the regular repair on damaged bridges has demonstrated to be playing a crucial role to seismic resilience of *RNs*. Moreover, without losses of generality, the case-study outcome shows that post-shock rapid responses can decrease the restoration duration of critical connectivity by up to 96.8%. Therefore, it can be concluded that a well-planned rapid response can serve as a promising and viable pathway towards future resilient *RNs*.

It is noteworthy to mention that, post-shock recovery process of *RNs* is rather dynamic and stochastic. Notwithstanding the effectiveness associated with the reparability-oriented rapid responses on severely-damaged bridges, here expressed as a function of the span, more sophisticated and adaptive strategies need to be developed to better ameliorate the seismic resilience of *RNs*, in particular, throughout the immediate aftermath of earthquakes.

Furthermore, as shown in this study, from the perspective of hazard preparedness, it is strategically crucial for effective disaster management of communities in earthquake-prone areas to hoard sufficient rapid response resources (*e.g.* manoeuvrable vehicles that can be deployed in mountainous or harsh regions, prefabricated ramps, self-propelled cranes, and etc.) at all times, allowing for emergency response squads to fulfil their restoration objective, in an expeditious way. The total expected socio-economic losses with regard to the hazard-impacted community can be significantly reduced as well, owing to those rapid response endeavors.

Lastly, it shall also be highlighted that, despite the resilience improvement of *RNs* that post-shock rapid response could bring about, cost analysis on such a new approach has been meagre, so far. Hence, granular data needs be to collected from communities with different socio-economic context, and corresponding, adaptive models could be therefore developed. Based on such models, investment on rapid response policies can be weighted, in probabilistic terms, against policies of seismic upgrading of bridges on such networks, by accounting for the consequences of traffic disruptions (Stergiou and Kiremidjian 2010), emergency rescues (Ceferino et al. 2020), and the recovery of other *CISs* across the community of interest, throughout the immediate aftermath of damaging earthquakes. Accordingly, a comprehensive, budget-based optimization framework can be established, where the investment on rapid response, long-term reconstruction and the pre-shock retrofit (Zanini et al. 2016) can all be put into perspective, to better inform the decision-making and risk governance of urban communities imperilled by future catastrophic earthquakes.

Acknowledgement

The contribution of Mr. Zhou Mei, a former graduate student at *University College London*, is appreciated. Besides, the financial support from the European Union's *Horizon 2020 Research and Innovation Program*, with the grant number of *821046*, *Towards more earthquake-resilient urban societies through a multi-sensor-based information system enabling earthquake forecasting, early warning and rapid response actions (TURNKey)*, is also gratefully acknowledged.

References

[1] Aki, H. (2017). Demand-side resiliency and electricity continuity: Experiences and lessons learned in Japan. *Proceedings of the IEEE* 105(7): 1443-1455.

[2] Alessandri, S, Giannini, R, and Paolacci, F. (2013). Aftershock risk assessment and the decision to open traffic on bridges. *Earthquake Engineering & Structural Dynamics* 42(15): 2255-2275.

[3] Argyroudis, S. A., Mitoulis, S. A., Hofer, L., Zanini, M. A., Tubaldi, E., and Frangopol, D. M. (2020). Resilience assessment framework for critical infrastructure in a multi-hazard environment: Case study on transport assets. *Science of The Total Environment* 714: 136854.

[4] Aydin, N. Y., Duzgun H. S., Heinimann, H. R., Wenzel, F., and Gnyawali, K. R. (2018). Framework for improving the resilience and recovery of transportation networks under geohazard risks. *International Journal of Disaster Risk Reduction* 31: 832-843.

[5] Blake, D. M., Stevenson, J., Wotherspoon, L., Ivory, V., and Trotter, M. (2019). The role of data and information exchanges in transport system disaster recovery: A New Zealand case study. *International Journal of Disaster Risk Reduction* 39:101124.

[6] Bocchini, P, and Frangopol, D. M. (2012). Restoration of bridge networks after an earthquake: Multicriteria intervention optimization. *Earthquake Spectra* 28(2): 427-455.

[7] Brandes, U. (2001). A faster algorithm for betweenness centrality. *Journal of Mathematical Sociology* 25(2): 163-177.

[8] Bruneau, M., Chang, S. E., Eguchi, R. T., Lee, G. C., O'Rourke, T. D., Reinhorn, A. M., Shinozuka, M., Tierney, K., Wallace, W. A., and Winterfeldt, D. V. (2003). A framework to quantitatively assess and enhance the seismic resilience of communities. *Earthquake Spectra* 19(4): 733-752.

[9] Campbell, K. W., and Bozorgnia, Y. (2008). NGA ground motion model for the geometric mean horizontal component of PGA, PGV, PGD and 5% damped linear elastic response spectra for periods ranging from 0.01 to 10 s. *Earthquake Spectra* 24 (1): 139-171.

[10] Ceferino, L., Reiser, J. M., Kiremidjian A., Deierlein, G., and Bambarén C. (2020). Effective plans for hospital system response to earthquake emergencies. *Nature Communications* 11: 4325.

[11] D'Ayala, D. et al. (2019). *The M_W 6.2 Amatrice, Italy Earthquake of 24th August 2016*. A field report by Earthquake Engineering Field Investigation Team (*EEFIT*). *https://www.istructe.org/IStructE/media/Public/Resources/report-eefit-mission-italy-20190501.pdf*

[12] Decò, A., Bocchini, P. and Frangopol, D. M. (2013). A probabilistic approach for the prediction of seismic resilience of bridges. *Earthquake Engineering & Structural Dynamics* 42(10): 1469-1487.

[13] Do, M., and Jung, H. (2018). Enhancing road network resilience by considering the performance loss and asset value. *Sustainability* 10(11): 4188.

[14] Dong, Y., and Frangopol, D. M. (2015). Risk and resilience assessment of bridges under mainshock and aftershocks incorporating uncertainties. *Engineering Structures* 83: 198-208.

[15] Durante, M. G., Sarno, L. D., Zimmaro, P., and Stewart, J. P. (2018). Damage to roadway infrastructure from 2016 Central Italy Earthquake sequence. *Earthquake Spectra* 34(4): 1721-1737.

[16] Fakharifar, M., Chen, G. D., Wu, C. L., Shamsabadi, A., ElGawady, M. A., and Dalvand, A. (2016). Rapid repair of earthquake-damaged *RC* columns with prestressed steel jackets. *Journal of Bridge Engineering* 21(4): 04015075.

[17] Fraioli, G., Gosavi, A., and Sneed, L. (2021). Strategic implications for civil infrastructure and logistical support systems in post-earthquake disaster management: The case of St. Louis. *IEEE Engineering Management Review* 49(1): 165-173.

[18] García-Fernández, M., Gehl, P., Jiménez, M. J., and D'Ayala, D. (2019). Modelling Pan-European ground motions for seismic hazard applications. *Bulletin of Earthquake Eng*ineering 17(6): 2821-2840.

[19] Gehl, P., and D'Ayala, D. (2016). Development of Bayesian networks for the multi-hazard fragility assessment of bridge systems. *Structural Safety* 60: 37-46.

[20] Gehl, P., and D'Ayala, D. (2018). System loss assessment of bridge networks accounting for multi-hazard interactions. *Structure and Infrastructure Engineering* 14 (10): 1355-1371.

[21] Gomez, C., and Baker, J. W. (2019). An optimization-based decision support framework for coupled pre- and post-earthquake infrastructure risk management. *Structural Safety* 77: 1-9.

[22] Guidotti, R., Gardoni, P., and Chen, Y. (2017). Network reliability analysis with link and nodal weights and auxiliary nodes. *Structural Safety* 65: 12-26.

[23] Guidotti, R., Gardoni, P., and Rosenheim, N. (2019). Integration of physical infrastructure and social systems in communities' reliability and resilience analysis. *Reliability Engineering & System Safety* 185: 476-492.

[24] Gyawali, S., Tiwari, S. R., Bajracharya, S. B., and Skotte, H. N. (2020). Promoting sustainable livelihoods: An approach to postdisaster reconstruction. *Sustainable Development* 28(4): 626-633.

[25] Hashash, Y. M. A., Tiwari, B., Moss, R. E. S., Asimaki, D., Clahan, K. B., Kieffer, D. S., Dreger, D. S., Macdonald, A., Madugo, C. M., Mason, H. B., Pehlivan, M., Rayamajhi, D., Acharya, I., and Adhikari, B. (2015). Geotechnical field reconnaissance: Gorkha (Nepal) Earthquake of April 25, 2015 and related shaking sequence. Geotechnical Extreme Event Reconnaissance, GEER Association Report No. GEER-040. *http://www.geerassociation.org/* (last accessed March 2021).

[26] Hassan, E. M., and Mahmoud, H. (2020). An integrated socio-technical approach for post-earthquake recovery of interdependent healthcare system. *Reliability Engineering & System Safety* 201: 106953.

[27] Helbing, D. (2013). Globally networked risks and how to respond. *Nature* 497(7447): 51-59.

[28] Hosseini, S., Barker, K., and Ramirez-Marquez, J. E. (2016). A review of definitions and measures of system resilience. *Reliability Engineering & System Safety* 145: 47-61.

[29] Kilanitis, I., and Sextos, A. (2019). Integrated seismic risk and resilience assessment of roadway networks in earthquake prone areas. *Bulletin of Earthquake Engineering* 17(1): 181-210.

[30] Kröger, W., and Zio, E. (2011). *Vulnerable systems*. London: Springer.

[31] Lekkas, E., Andreadakis, E., Alexoudi, V., Kapourani, E., and Kostaki, I. (2012). The M_w = 9.0 Tohoku Japan earthquake (March 11, 2011) tsunami impact on structures and infrastructure. *Proceedings of the 15th World Conference on Earthquake Engineering, Lisbon, Portugal*.

[32] Long, A., Kirkpatrick, J., Gupta, A., Nanukuttan, S., and McPolin, D. (2013). Rapid construction of arch bridges using the innovative *FlexiArch*. *Proceedings of the ICE-Bridge Engineering* 166(3): 143-153.

[33] Merschman, E, Doustmohammadi, M, Salman A. M., and Anderson, M. (2020). Postdisaster Decision Framework for Bridge Repair Prioritization to Improve Road Network Resilience. *Transportation Research Record* 2674(3):81-92.

[34] Norton, G. H. (2020). *Rapid Repair of seismically vulnerable bridge columns following earthquake induced damage*. Master's Project Reports, Portland State University, United States.

[35] Ouyang, M., Dueñas-Osorio, L., and Min, X. (2012). A three-stage resilience analysis framework for urban infrastructure systems. *Structural Safety* 36-37: 23-31.
[36] Ouyang, M. (2014). Review on modeling and simulation of interdependent critical infrastructure systems. *Reliability Engineering and System Safety* 121: 43-60.
[37] Parks, J. E., Brown, D. N., Ameli, M. J., and Pantelides, C. P. (2016). Seismic repair of severely damaged precast reinforced concrete bridge columns connected with grouted splice sleeves. *ACI Structural Journal* 113(3): 615-626.
[38] Reasenberg, P. A., and Jones, L. M. (1994). Earthquake aftershocks: Update. *Science* 265(5176): 1251-1252.
[39] Schanack, F., Valdebenito, G., and Alvial, J. (2012). Seismic damage to bridges during the 27 February 2010 magnitude 8.8 Chile Earthquake. *Earthquake Spectra* 28(1): 301-305.
[40] Shao, Z., Ma, Z., Liu, S., and Lv, T. (2018). Optimization of a traffic control scheme for a post-disaster urban road network. *Sustainability* 10(1): 68.
[41] Shinozuka, M., Feng, M. Q., Kim, H. K., Uzawa, T., and Ueda, T. (2003). *Statistical analysis of fragility curves*. Technical report MCEER-03-0002. http://shinozuka.eng.uci.edu/Pdf/RepFrag.pdf
[42] Smith, K. (2013). *Environmental hazards: Assessing risk and reducing Disaster (6th Edition)*. Routledge.
[43] SPUR (San Francisco Planning and Urban Research Association). (2009). The resilient city: Defining what San Francisco needs from its seismic mitigation polices. http://resilience.abag.ca.gov/wp-content/documents/resilience/toolkit/Defining%20What%20San%20Francisco%20Needs%20from%20its%20Seismic%20Mitigation%20Policies.pdf. (last accessed September 13, 2021).
[44] Stergiou, E., and Kiremidjian, A. (2010). Risk assessment of transportation systems with network functionality losses. *Structure and Infrastructure Engineering* 6(1-2): 111-125.
[45] Sun, L., Didier, M., Delé, E., and Stojadinovic, B. (2015). Probabilistic demand and supply resilience model for electric power supply system under seismic hazard. *Proceedings of the 12th International Conference on Applications of Statistics and Probability in Civil Engineering (ICASP12), Vancouver, Canada, July, 12-15*.
[46] Sun, L. (2017). Modeling the seismic resilience of electric power supply systems. Ph.D. Thesis, ETH Zurich, Switzerland.
[47] Sun, L., Stojadinovic, B., and Sansavini, G. (2019a). Resilience evaluation framework for integrated civil infrastructure-community systems under seismic hazard. *ASCE Journal of Infrastructure Systems* 25 (2): 04019016.
[48] Sun, L., Stojadinovic, B., and Sansavini, G. (2019b). Agent-based recovery model for seismic resilience evaluation of electrified communities. *Risk Analysis* 7(39): 1597-1614.
[49] Sun, Z., Li, H., Bi, K., Si, B., and Wang, D. (2017). Rapid repair techniques for severely earthquake-damaged circular bridge piers with flexural failure mode. *Earthquake Engineering and Engineering Vibration*16(2): 415-433.
[50] Woessner, J., Danciu, L., Kaestli, P., and Monelli, D. (2013). *D6.6-Database of seismogenic zones, Mmax, earthquake activity rates, ground motion attenuation relations and associated logic trees*. Deliverable of the Seismic Hazard Harmonization in Europe (SHARE) project. http://www.efehr.org/export/sites/efehr/.galleries/dwl_europe2013/D6-6_SHAREopt.pdf_2063069299.pdf
[51] Wu, Y., Hou, G., and Chen, S. (2021). Post-earthquake resilience assessment and long-term restoration prioritization of transportation network. *Reliability Engineering & System Safety* 211: 107612.
[52] Yeh, F. Y., Chang, K. C., Sung, Y. C., Hung, H. H., and Chou, C. C. (2015). A novel composite bridge for emergency disaster relief: Concept and verification. *Composite Structures* 127: 199-210.
[53] Zampieri, P. (2014). *Simplified seismic vulnerability assessment of masonry arch bridges*. Ph.D.

Thesis, University of Trento, Italy.
[54] Zanini, M. A., Faleschini, F., and Pellegrino, C. (2016). Cost analysis for maintenance and seismic retrofit of existing bridges. *Structure and Infrastructure Engineering* 12(11): 1411-1427.
[55] Zhang, W., Wang, N., and Nicholson, C. (2017). Resilience-based post disaster recovery strategies for road-bridge networks. *Structure and Infrastructure Engineering* 13(11): 1404-1413.
[56] Zhao, B., and Taucer, F. (2010). Performance of infrastructure during the May 12, 2008 Wenchuan Earthquake in China. *Journal of Earthquake Engineering* 14(4): 578-600.
[57] Zhao, T., and Sun, L. (2021). Seismic resilience assessment of critical infrastructure-community systems considering looped interdependences. *International Journal of Disaster Risk Reduction* 59: 102246.

Appendix

Table 3. List of the abbreviations in the manuscript

Abbreviation	Nomenclature
CIS	Critical Infrastructure System
ABM	Agent-based model
IAoE	Immediate aftermath of earthquake
PGA	Peak Ground Acceleration
RN	Road network
RRbR	Rapid Response-based Resilience
PFB	Percentage of functional bridges
NLCP	Normalized length of critical path

Table 4. List of the parameters

Abbreviation	Physical term
$R_{r,j}$	The time to deliver the rapid response to bridge *j*
$T_{r,j}$	The time to arrive at bridge *j*
$SD_{r,j}$	The shortest distance to reach bridge *j*
E_r	Efficiency of rapid response
V_r	The travelling speed of rapid response *Agent*
R_i	The time to deliver the full repair to bridge *i*
T_i	The time to arrive at bridge *i*
SD_i	The shortest distance to reach bridge *i*
E_m	Repair efficiency of bridges with minor damage
V_m	The travelling speed of the *Agent* delivering repair to bridges with minor damage